PROJECT REPORT: FRACTURE FIXATION FEA SIMULATION

Wenye Xiong
2023533141
xiongwy2023@shanghaitech.edu.cn

Renyi Yang
2023533030
yangry2023@shanghaitech.edu.cn

Zijian Li
2023533185
lizj2023@shanghaitech.edu.cn

June 15, 2025

ABSTRACT

This project utilizes Finite Element Analysis to investigate the critical biomechanical phenomenon of "stress transfer" during the fracture healing process. A 2D computational model of a "bone-fixator" system was developed to analyze how varying fixator stiffness influences stress redistribution among the bone, fixator, and nascent callus. Furthermore, the study examines the resultant strain environment within the fracture gap as the bone progressively regains its load-bearing capacity. By simulating the gradual maturation of callus tissue under different fixator rigidities, this research aims to elucidate the complex interplay between fixator mechanical properties and the evolving biomechanical conditions at the fracture site. The findings are intended to provide valuable insights for optimizing fracture fixation strategies to enhance healing outcomes.

Keywords Finite element analysis · Fracture fixation · Small deformation theory · Stress transfer · Fixator stiffness · Bone healing

1 Introduction

Fracture healing is a dynamic biological process profoundly influenced by its mechanical environment. A key aspect of successful osteosynthesis is the gradual transfer of physiological loads from the orthopedic fixator back to the healing bone as it regenerates and regains structural integrity. This "stress transfer" mechanism is essential for stimulating bone formation and remodeling. This project employs Finite Element Analysis, a powerful computational tool, to model and investigate this critical stress transfer phenomenon. Specifically, we developed a simplified 2D "bone-fixator" system to explore how variations in fixator stiffness affect the distribution of mechanical stresses within the bone, the fixator itself, and the developing callus tissue at the fracture site. Concurrently, we analyze the mechanical strain experienced within the fracture gap, a crucial parameter known to modulate cellular activity during healing. By simulating the progressive stiffening of the callus over time, this study aims to provide a clearer understanding of how fixator design choices impact the biomechanical milieu of a healing fracture, which is vital for optimizing clinical treatments and minimizing complications such as delayed union or non-union.

2 Overview of existing work

Finite Element Analysis has become an indispensable tool in biomechanical research, particularly in orthopedics, for simulating and analyzing the behavior of biological structures and medical devices under diverse physiological conditions. It plays a crucial role in understanding fracture mechanics, optimizing implant design, and predicting the efficacy of various fracture fixation strategies [Lewis et al., 2021]. Traditional evaluative methods, such as in vitro experiments and clinical trials, while essential, often present limitations regarding cost, duration, and the feasibility of

extensive parametric studies. FEA offers a robust complementary approach, enabling detailed, non-invasive examination of complex stress and strain distributions within bone-implant constructs.

A central concept in fracture fixation is "stress shielding," where an overly rigid fixation device bears a disproportionate share of the applied load, thereby reducing the mechanical stimulus transmitted to the healing bone. While a degree of stress shielding is necessary for initial fracture stability, excessive shielding can impede natural bone healing by inhibiting callus formation and its subsequent remodeling into lamellar bone. Conversely, insufficient stability due to overly flexible fixation can lead to excessive interfragmentary motion, potentially resulting in hypertrophic non-union or fixation failure. Consequently, achieving an optimal mechanical environment that balances stability with appropriate mechanical stimulation is paramount for successful fracture healing.

Recent advancements in computational biomechanics have focused on developing sophisticated models that can simulate the mechanobiological processes governing fracture healing. These models often incorporate time-dependent material properties for the healing callus and consider the influence of mechanical stimuli, such as strain or hydrostatic stress, on tissue differentiation pathways [Morgan et al., 2024]. Parametric studies using FEA are instrumental in investigating how factors like fixator stiffness, fracture gap size, loading conditions, and healing progression affect the stress transfer dynamics from the fixator to the bone.

3 Integration of the content of the course

This study leverages Finite Element Analysis to model the complex stress redistribution dynamics that occur during fracture healing. The model incorporates time-dependent material properties for the healing callus and facilitates parametric studies on the influence of fixator stiffness.
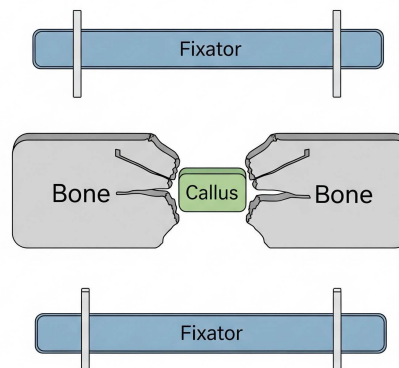
3.1 Problem Definition

Figure 1: Model

- **Domain Type**: Non-homogeneous, linear elastic body subjected to quasi-static loading, featuring time-varying material properties (specifically, the elastic modulus of the callus).

- **Computational Model**: A 2D plane stress representation of a "bone-fixator" system, incorporating a healing fracture gap (callus). The domain is discretized using quadrilateral finite elements.

- **Key Features Investigated**:

  - Simulation of the progressive stress transfer from the fixator to the bone tissue as callus stiffness increases with healing.

  - Parametric analysis of the system's response under varying fixator stiffness conditions.

  - Quantitative evaluation of stress shielding effects imparted by the fixator.

  - Monitoring and analysis of the evolution of strain within the fracture gap (callus region).

3.2 Mathematical Model

3.2.1 Mechanical Framework

The problem is formulated within the context of linear elasticity, considering time-dependent material properties. The constitutive relationship is given by:

$$\boldsymbol{\sigma}^{(t)} = \mathbf{D}^{(t)} \boldsymbol{\varepsilon}$$

where:

- $\boldsymbol{\sigma}^{(t)}$ represents the Cauchy stress tensor at a given healing time point t.
- $\boldsymbol{\varepsilon}$ is the small strain tensor, defined as $\varepsilon_{ij} = \frac{1}{2}(u_{i,j} + u_{j,i})$, where u denotes the displacement field.
- $\mathbf{D}^{(t)}$ is the plane stress constitutive matrix, which can vary with time due to callus maturation:

$$\mathbf{D} = \frac{E}{1 - \nu^2} \begin{bmatrix} 1 & \nu & 0 \\ \nu & 1 & 0 \\ 0 & 0 & \frac{1-\nu}{2} \end{bmatrix}$$

3.2.2 Material Property Evolution

The material properties for the different components are defined as follows:

$$\text{Bone tissue (cortical)} : E_{bone} = 18 \text{ GPa}, \nu = 0.3 \text{ (assumed constant)}$$
$$\text{Fixator} : E_{fixator} \in \{35, 70, 140\} \text{ GPa (parametrically varied)}$$
$$\text{Callus} : E_{callus}^{(t)} = E_0 + \frac{t}{t_{max}}(E_{final} - E_0)$$
$$\text{where initial modulus } E_0 = 0.1 \text{ GPa (soft tissue)},$$
$$\text{and final modulus } E_{final} = 18 \text{ GPa (mature bone)}.$$
$$t \text{ represents the current healing step, and } t_{max} \text{ is the total number of steps.}$$

3.2.3 Fracture Interface Modeling

The fracture gap, filled with healing callus, is modeled as a distinct region characterized by:

- An initial width $w_{frac} = 10$ mm, centrally located within the bone segment.
- Time-dependent material properties ($E_{callus}^{(t)}$) simulating biological healing and stiffening.
- Fracture gap strain (ε_{gap}) is quantified as the average axial strain within the elements comprising the callus region, derived from the computed displacement field.

3.3 Finite Element Implementation

The FE model employs bilinear quadrilateral elements (Q4), whose width is $2m$, height is $2l$.

3.3.1 Nodal Displacement Matrix

$$\mathbf{d} = \begin{bmatrix} d_1 \\ d_2 \\ d_3 \\ d_4 \end{bmatrix} = \begin{bmatrix} u_1 \\ v_1 \\ u_2 \\ v_2 \\ u_3 \\ v_3 \\ u_4 \\ v_4 \end{bmatrix}$$

3.3.2 Selection of Displacement Functions

$$\begin{cases} u(x,y) = a_1 + a_2 x + a_3 y + a_4 xy \\ v(x,y) = b_1 + b_2 x + b_3 y + b_4 xy \end{cases}$$

Eliminating a, b yields

$$\begin{cases} u(x,y) = \frac{1}{4bh}\left[(m-y)(l-x)u_1 + (m+y)(l-x)u_2 + (m+y)(l+x)u_3 + (m-y)(l+x)u_4\right] \\ v(x,y) = \frac{1}{4bh}\left[(m-y)(l-x)v_1 + (m+y)(l-x)v_2 + (m+y)(l+x)v_3 + (m-y)(l+x)v_4\right] \end{cases}$$

$$\psi = \begin{bmatrix} u(x,y) \\ v(x,y) \end{bmatrix} = [N]\{d\}$$

The shape functions are as follows:

$$\mathbf{N} = \begin{bmatrix} N_1 & 0 & N_2 & 0 & N_3 & 0 & N_4 & 0 \\ 0 & N_1 & 0 & N_2 & 0 & N_3 & 0 & N_4 \end{bmatrix}$$

where

$$\begin{array}{ll} N_1 = \frac{1}{4bh}(m-y)(l-x) & N_2 = \frac{1}{4bh}(m+y)(l-x) \\ N_3 = \frac{1}{4bh}(m+y)(l+x) & N_4 = \frac{1}{4bh}(m-y)(l+x) \end{array}$$

3.3.3 Coordinate Transformation

To simplify calculations, the quadrilateral in the $x-y$ coordinate system is transformed into a square centered at the origin with a side length of 2 in the $\xi - \eta$ coordinate system. The transformation relationship is:

$$\begin{cases} x = x_0 + m\xi \\ y = y_0 + l\eta \end{cases}$$

where x_0, y_0 are the coordinates of the element center. Let the coordinate transformation from $x-y$ to $\xi - \eta$ be defined as:

$$\begin{cases} x = a_1 + a_2\xi + a_3\eta + a_4\xi\eta \\ y = b_1 + b_2\xi + b_3\eta + b_4\xi\eta \end{cases}$$

Given the four node coordinates $(1,1), (1,-1), (-1,-1), (-1,1)$ in the $\xi - \eta$ coordinate system, corresponding to $(x_1, y_1), (x_2, y_2), (x_3, y_3), (x_4, y_4)$ in the $x-y$ coordinate system, the values of $a_1, a_2, a_3, a_4, b_1, b_2, b_3, b_4$ can be determined. Thus, the coordinate transformation from $\xi - \eta$ to $x-y$ is:

$$\begin{cases} x = \frac{1}{4}\left[(1-\xi)(1-\eta)x_1 + (1+\xi)(1-\eta)x_2 + (1+\xi)(1+\eta)x_3 + (1-\xi)(1+\eta)x_4\right] \\ y = \frac{1}{4}\left[(1-\xi)(1-\eta)y_1 + (1+\xi)(1-\eta)y_2 + (1+\xi)(1+\eta)y_3 + (1-\xi)(1+\eta)y_4\right] \end{cases}$$

That is,

$$\begin{bmatrix} x \\ y \end{bmatrix} = \mathbf{Nd} = \begin{bmatrix} N_1 & 0 & N_2 & 0 & N_3 & 0 & N_4 & 0 \\ 0 & N_1 & 0 & N_2 & 0 & N_3 & 0 & N_4 \end{bmatrix} \begin{bmatrix} x_1 \\ y_1 \\ x_2 \\ y_2 \\ x_3 \\ y_3 \\ x_4 \\ y_4 \end{bmatrix}$$

where

$$\begin{array}{ll} N_1 = \frac{1}{4}(1-\xi)(1-\eta) & N_2 = \frac{1}{4}(1+\xi)(1-\eta) \\ N_3 = \frac{1}{4}(1+\xi)(1+\eta) & N_4 = \frac{1}{4}(1-\xi)(1+\eta) \end{array}$$

3.3.4 Stress/Strain Calculation

The stress matrix is:

$$\sigma = \begin{bmatrix} \sigma_x \\ \sigma_y \\ \tau_{xy} \end{bmatrix} = \mathbf{D}\epsilon$$

The strain matrix is:

$$\epsilon = \begin{bmatrix} \epsilon_x \\ \epsilon_y \\ \gamma_{xy} \end{bmatrix} = \begin{bmatrix} \frac{\partial u}{\partial \xi} \\ \frac{\partial v}{\partial \eta} \\ \frac{\partial u}{\partial \eta} + \frac{\partial v}{\partial \xi} \end{bmatrix} = \begin{bmatrix} \frac{\partial ()}{\partial \xi} & 0 \\ 0 & \frac{\partial ()}{\partial \eta} \\ \frac{\partial ()}{\partial \eta} & \frac{\partial ()}{\partial \xi} \end{bmatrix} \begin{bmatrix} u \\ v \end{bmatrix}$$

Since

$$\begin{cases} \frac{\partial f}{\partial \xi} = \frac{\partial f}{\partial \xi} \cdot \frac{\partial \xi}{\partial \xi} + \frac{\partial f}{\partial \eta} \cdot \frac{\partial \eta}{\partial \xi} \\ \frac{\partial f}{\partial \eta} = \frac{\partial f}{\partial \xi} \cdot \frac{\partial \xi}{\partial \eta} + \frac{\partial f}{\partial \eta} \cdot \frac{\partial \eta}{\partial \eta} \end{cases}$$

Therefore,

$$\begin{cases} \frac{\partial f}{\partial \xi} = \frac{1}{|J|} \left[\frac{\partial \eta}{\partial \eta} \frac{\partial f}{\partial \xi} - \frac{\partial \eta}{\partial \xi} \frac{\partial f}{\partial \eta} \right] \\ \frac{\partial f}{\partial \eta} = \frac{1}{|J|} \left[\frac{\partial \xi}{\partial \xi} \frac{\partial f}{\partial \eta} - \frac{\partial \xi}{\partial \eta} \frac{\partial f}{\partial \xi} \right] \end{cases}$$

where $|J|$ is the Jacobian determinant:

$$|J| = \begin{vmatrix} \frac{\partial \xi}{\partial \xi} & \frac{\partial \xi}{\partial \eta} \\ \frac{\partial \eta}{\partial \xi} & \frac{\partial \eta}{\partial \eta} \end{vmatrix}$$

Thus,

$$\{B\} = \frac{1}{|J|} \begin{bmatrix} B_1 & B_2 & B_3 & B_4 \end{bmatrix}$$

where

$$[B_i] = \begin{bmatrix} \frac{\partial N_i}{\partial \xi} & 0 \\ 0 & \frac{\partial N_i}{\partial \eta} \\ \frac{\partial N_i}{\partial \eta} & \frac{\partial N_i}{\partial \xi} \end{bmatrix}$$

3.3.5 Element Stiffness Matrix

Element stiffness matrices, $\mathbf{k}^e$, is computed using $2{\times}2$ Gauss quadrature:

$$\mathbf{k}^e = \int_{-1}^{1} \int_{-1}^{1} \mathbf{B}^T(\xi, \eta) \mathbf{D} \mathbf{B}(\xi, \eta) |\mathbf{J}(\xi, \eta)| \, t_{thickness} \, d\xi d\eta$$

$$\approx \sum_{i=1}^{2} \sum_{j=1}^{2} w_i w_j \mathbf{B}^T(\xi_i, \eta_j) \mathbf{D} \mathbf{B}(\xi_i, \eta_j) |\mathbf{J}(\xi_i, \eta_j)| \, t_{thickness}$$

where integration points are at $\xi_i, \eta_j = \pm \frac{1}{\sqrt{3}}$ with weights $w_i = w_j = 1$, and $t_{thickness}$ is the out-of-plane thickness for plane stress.

3.3.6 Postprocessing and Analysis

Key metrics for evaluating the biomechanical performance include:

- Stress shielding: Assessed by comparing average Von Mises stresses in the fixator versus those in the bone and callus. A formal ratio (e.g., $\sigma_{avg,fixator}/\sigma_{avg,bone}$) can also be derived.

- Fracture gap strain evolution: Tracking the average axial strain in the callus region over the simulated healing period.

- Stress distribution patterns: Analyzing Von Mises stress contours within the callus, bone, and fixator.

- Load transfer dynamics: Observing how the distribution of load between the fixator and the bone-callus construct changes as healing progresses.

Visualization techniques employed:

- Contour plots illustrating the spatial distribution of Von Mises stress.

- Time-history plots showing the evolution of average stresses in different regions.

- Comparative plots to highlight differences across the parametric studies of fixator stiffness.

4 Our own contribution

Our primary contribution in this project is the systematic development and application of a parametric Finite Element Analysis model designed to investigate the influence of varying fixator stiffness on stress transfer mechanisms and fracture gap biomechanics throughout a simulated bone healing process. The key facets of our contribution are:

4.1 Parametric Study of Fixator Stiffness

We conducted a systematic investigation of the fixator to represent three distinct clinical scenarios, allowing for a direct comparison of their biomechanical effects:

- **Flexible Fixator**: $E_{fixator} = 35$ GPa (representative of more compliant materials or designs).

- **Standard Fixator**: $E_{fixator} = 70$ GPa (representative of moderately stiff fixators, e.g., certain aluminum alloys).

- **Rigid Fixator**: $E_{fixator} = 140$ GPa (representative of stiffer materials or more robust designs, e.g., some titanium alloys or stainless steel constructs, scaled for 2D comparison).

This parametric approach enables a direct comparison of how fixator stiffness modulates the biomechanical environment of the healing fracture.

4.2 Time-Dependent Callus Healing Model

A progressive healing model was implemented where the modulus of the callus (E_{callus}) increases linearly over 20 discrete simulation steps. This simulates the gradual stiffening of the fracture site, from an initial soft tissue-like stiffness ($E_{callus}^{initial} = 0.1$ GPa) to that of mature, remodeled bone ($E_{callus}^{final} = 18$ GPa).

4.3 Quantitative Analysis of Biomechanical Parameters

For each simulation step and each fixator stiffness configuration, we computed and tracked key biomechanical indicators critical for understanding healing progression:

- **Average Von Mises Stress**: Calculated independently for the bone, callus, and fixator regions. This metric helps quantify the stress distribution, load sharing, and the extent of stress shielding.

- **Fracture Gap Strain**: Defined as the average axial strain across the callus region, this parameter is a critical factor known to influence tissue differentiation and the overall healing outcome.

4.4   Development of a Reusable FEA Simulation Script

A comprehensive Python script was developed, leveraging NumPy for efficient numerical computations and Matplotlib for generating high-quality visualizations. This script automates the entire simulation pipeline:

- Assignment of material properties, including the time-dependent updates for the callus region.
- Assembly of the global stiffness matrix and application of appropriate boundary conditions and loads.
- Solution of the system of linear equations to obtain nodal displacements, followed by calculation of element stresses and strains.
- Automated post-processing to extract average stresses in defined regions and calculate the fracture gap strain.
- Generation of a suite of visualizations, including final stress distributions and gap strain evolution across different fixator stiffnesses.

This robust and automated framework allows for efficient exploration of various biomechanical parameters and alternative simulation scenarios.

5   Numerical results

The FEA simulations were executed for three distinct fixator stiffness configurations: Flexible (35 GPa), Standard (70 GPa), and Rigid (140 GPa). The fracture healing process was simulated across 20 discrete steps, characterized by a progressive increase in callus stiffness. Table 1 summarizes the key biomechanical parameters observed at the final healing step (Step 20), corresponding to full callus maturation (i.e., callus stiffness equals that of intact bone).

Table 1: Summary of Biomechanical Parameters at Full Callus Maturation (Simulation Step 20)

Fixator Group	Final Avg. Stress in Fixator (MPa)	Final Avg. Stress in Bone (MPa)	Final Avg. Stress in Callus (MPa)	Final Avg. Gap Strain ($\mu\varepsilon$)
Flexible Fixator (35 GPa)	48.89	25.46	25.35	1.41
Standard Fixator (70 GPa)	64.92	17.57	16.98	0.94
Rigid Fixator (140 GPa)	77.85	11.30	10.23	0.57

Note: Stresses reported are average Von Mises stresses within the respective regions. Gap strain represents the average axial strain in the callus region. Values are derived from the simulation output, with stresses converted from Pa to MPa and strain from absolute values to microstrain for enhanced readability.

5.1   Interpretation of Results

The numerical results provide quantitative insights into the influence of fixator stiffness on the mechanical environment of a healing fracture.

Stress Distribution and Stress Shielding: As the stiffness of the fixator increases from Flexible (35 GPa) to Rigid (140 GPa), distinct trends emerge:

- The average Von Mises stress borne by the **fixator** increases substantially (from 48.89 MPa for the Flexible Fixator to 77.85 MPa for the Rigid Fixator). This is an anticipated outcome, as a stiffer fixator inherently attracts a larger proportion of the applied load.
- Conversely, the average Von Mises stress experienced by the **bone** tissue (adjacent to the callus) decreases markedly (from 25.46 MPa to 11.30 MPa). This clearly demonstrates an increased stress shielding effect with more rigid fixation; the stiffer fixator shields the bone from mechanical loading.
- Similarly, the average Von Mises stress within the fully matured **callus** also decreases with increasing fixator stiffness (from 25.35 MPa to 10.23 MPa), mirroring the trend observed in the adjacent bone.

These results quantitatively illustrate the phenomenon of stress shielding. While these specific values pertain to the final stage of healing (mature callus), the stress levels experienced by the developing callus during earlier, more compliant phases are critically important for mechanotransduction and guiding tissue differentiation.

Fracture Gap Strain: The average axial strain across the fracture gap (which, at Step 20, is mature callus) diminishes as fixator stiffness increases: 1.41 $\mu\varepsilon$ for the Flexible Fixator, 0.94 $\mu\varepsilon$ for the Standard Fixator, and 0.57 $\mu\varepsilon$ for the

Rigid Fixator. This indicates that more rigid fixation leads to reduced deformation (i.e., greater stability) at the fracture site. The magnitude of interfragmentary strain is a well-established critical factor influencing the pathway of bone healing (e.g., direct versus indirect healing, and the types of tissues formed). The very small strain values observed at Step 20 are expected for a fully healed bone segment under the simulated load. The evolution of this strain during the earlier, more critical phases of healing (when the callus is significantly softer) would be more directly indicative of the quality and type of healing response.

The detailed temporal evolution of these biomechanical parameters over the 20 simulated healing steps, along with illustrative stress contour plots, are available in the generated output files and visualizations produced by the Python simulation script. These comprehensive datasets provide a deeper understanding of the dynamic mechanobiological changes occurring throughout the simulated healing trajectory. For instance, plots depicting the "Stress Evolution" demonstrate how the proportion of load carried by the fixator versus the bone/callus system changes as the callus matures under each fixator stiffness condition. Similarly, "Fracture Gap Strain Evolution" plots trace the strain history at the fracture site. (as in figures 2, 3, and 4)

5.2   Visualizations

This section presents a detailed analysis of the graphical results obtained from the parametric finite element study. The findings illustrate the impact of varying fixator stiffness on the biomechanical environment at the fracture site, specifically concerning stress distribution and fracture gap strain dynamics. The core principle governing these phenomena is the dynamic load sharing between the implant and the maturing callus tissue throughout the simulated healing process.

Fracture Gap Strain Dynamics

The evolution of strain across the fracture gap serves as a primary indicator of the mechanical stability provided by each fixation construct. The results are presented in the left panels of Figures 2, 3, and 4

- **Initial Fracture Gap Strain:** At the commencement of the simulation (Step 0), a clear inverse relationship is observed between the stiffness of the fixator and the magnitude of the initial strain. The Flexible Fixator model yielded the highest initial strain (approx. 6.2×10^{-6}), whereas the Rigid Fixator model resulted in the lowest (approx. 1.7×10^{-6}). This outcome is consistent with mechanical principles, as a more rigid construct inherently provides greater stability, thereby restricting interfragmentary motion and reducing strain under a given load.

- **Temporal Evolution of Strain:** A consistent trend of decreasing strain over the simulation period is evident across all three models. This reduction is a direct consequence of the simulated healing, which is modeled by a progressive increase in the elastic modulus of the fracture callus. As the callus matures and its stiffness increases, the overall structural integrity of the bone-implant construct is enhanced. A stiffer construct deforms less under a constant applied load, leading to the observed decrease in fracture gap strain.
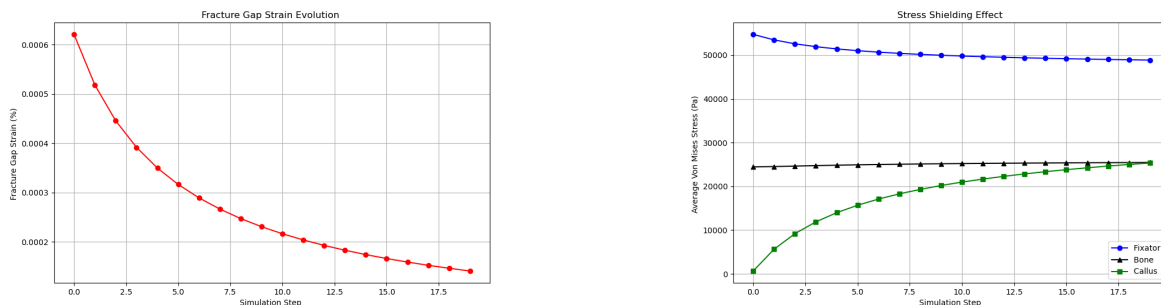

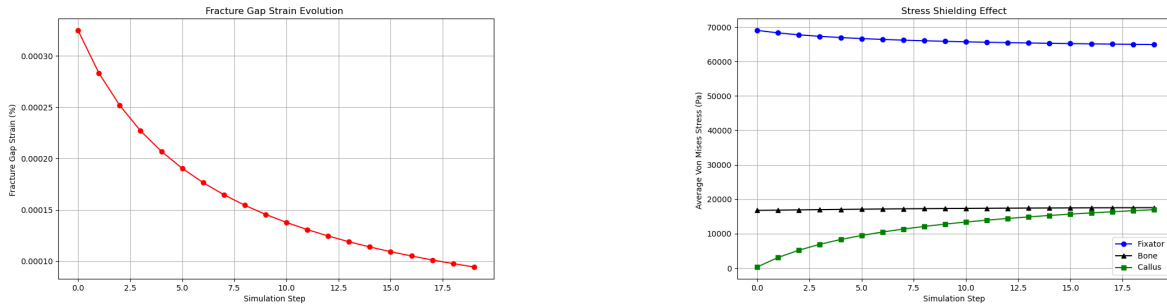Figure 2: Gap strain evolution (Left) and Stress evolution (Right) for Flexible Fixator

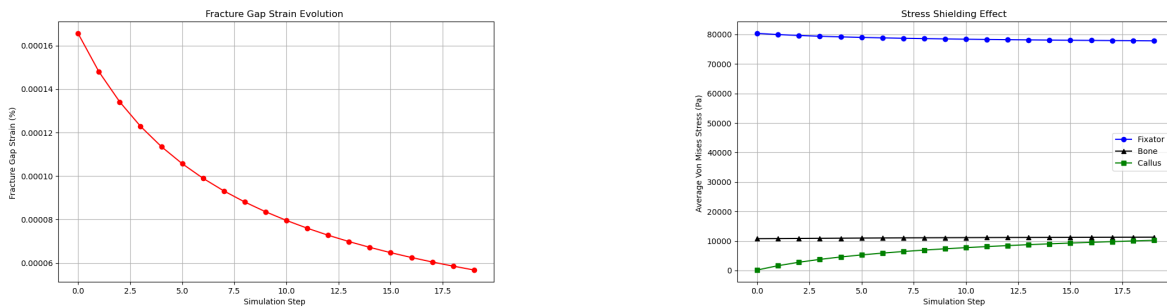Figure 3: Fracture gap strain evolution (Left) and Stress evolution (Right) for Standard Fixator

Figure 4: Fracture gap strain evolution (Left) and Stress evolution (Right) for Rigid Fixator

Stress Distribution and Dynamic Load Sharing

The analysis of stress evolution within each component—Fixator, Bone, and Callus—elucidates the mechanism of dynamic load sharing. These results are depicted in the right panels of Figures 2, 3, and 4 and the contour plots of Figure 5.

- **Initial Load Bearing State (Step 0):** In the initial state, the callus is modeled as mechanically incompetent due to its very low elastic modulus. Consequently, the external fixator bears the vast majority of the applied load. This is substantiated by the high initial stress levels in the fixator and near-zero stress in the callus, as shown in the line graphs. The contour plots in Figure 4 corroborate this, visualizing the callus region in deep blue (low stress) and the fixator in red (high stress).

- **Temporal Load Transfer:** A significant shift in load-bearing responsibility is observed as the simulation progresses. The average stress within the callus increases monotonically from nearly zero, while the stress in the fixator concurrently experiences a slight decrease. This demonstrates a direct transfer of mechanical load from the implant to the maturing callus.

- **The Effect of Fixator Stiffness and Stress Shielding:** The degree of load transfer is fundamentally governed by the fixator's stiffness, a phenomenon known as **stress shielding**. The Rigid Fixator maintains the highest stress levels throughout the simulation, effectively "shielding" the fracture site from mechanical stimuli by carrying a disproportionately large share of the load. This results in the lowest stress development within the callus. Conversely, the Flexible Fixator facilitates the greatest degree of load sharing, leading to the highest final stress in the callus, as the healing tissue is compelled to participate more actively in load bearing.

In summary, the simulation successfully demonstrates the fundamental biomechanical trade-offs inherent in fracture fixation. The stiffness of the selected implant dictates the initial mechanical environment, with more rigid fixators offering superior stability and lower initial gap strain. The healing process is characterized by a dynamic transfer of load from the implant to the maturing tissue. This investigation confirms that a more rigid fixator enhances the stress-shielding effect, while a more flexible fixator promotes load sharing. These findings are in strong agreement with established principles of fracture fixation biomechanics.
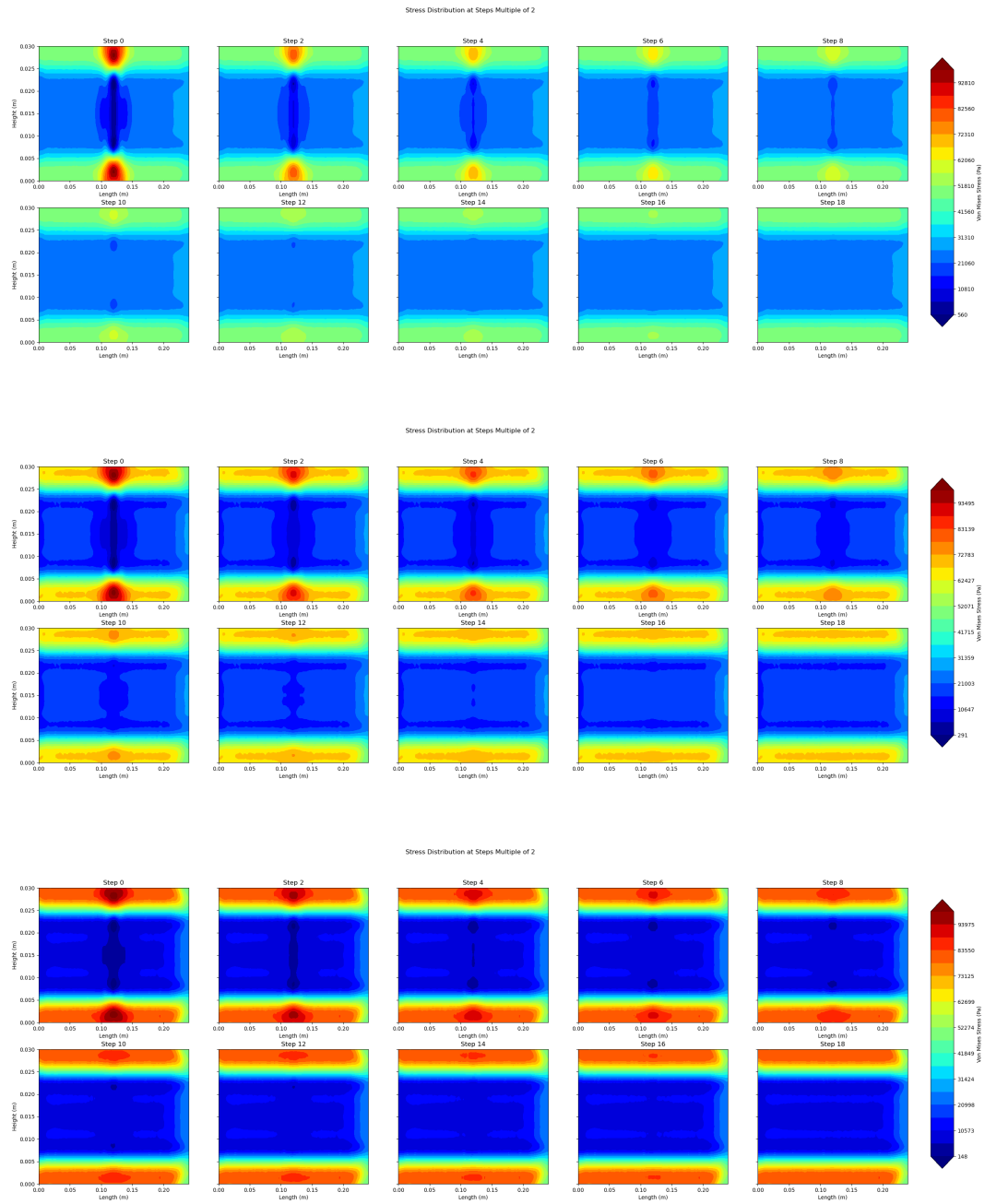
Figure 5: Stress distribution summary comparison for different fixator stiffnesses (Top: Flexible Fixator, Middle: Standard Fixator, Bottom: Rigid Fixator).

6   Conclusion

This project successfully developed and applied a 2D finite element model to simulate the biomechanics of fracture healing, specifically focusing on the influence of varying fixator stiffness. The parametric study yielded several key findings:

- Increasing fixator stiffness consistently led to higher stress concentrations within the fixator itself, coupled with correspondingly lower stresses in both the bone and the healing callus. This quantitatively demonstrates the well-known phenomenon of stress shielding.

- More rigid fixators resulted in significantly lower average strains within the fracture gap (callus region) throughout the simulated healing process, indicating greater mechanical stability at the fracture site.

These observations are in strong agreement with established biomechanical principles governing fracture fixation and healing. The flexible fixator (35 GPa) facilitated greater load sharing with the bone and callus, which could potentially promote more vigorous and uniform callus formation under appropriate conditions. Conversely, the rigid fixator (140 GPa) provided maximum initial stability but also induced the most pronounced stress shielding, which might delay bone remodeling if prolonged. The standard fixator (70 GPa) exhibited an intermediate biomechanical response.

The Python-based simulation framework developed for this project provides a versatile and reusable tool for conducting such parametric FEA studies. It enables the generation of detailed stress contour maps, plots of stress and strain evolution over time, and comparative analyses across different design parameters. Figure 6 offers a concise visual summary of the principal differences observed across the three fixator types at the culmination of the simulated healing period.

Future research could build upon this foundation by extending the model to three dimensions (3D), incorporating more sophisticated material models for bone and callus (e.g., anisotropic, poroelastic, or viscoelastic properties), and integrating mechanobiological algorithms to directly simulate tissue differentiation and healing progression based on local mechanical stimuli. Nonetheless, the current 2D model serves as a valuable educational and investigative tool for understanding the fundamental interplay between fixator mechanics, stress transfer, and the evolving mechanical environment of a healing fracture.
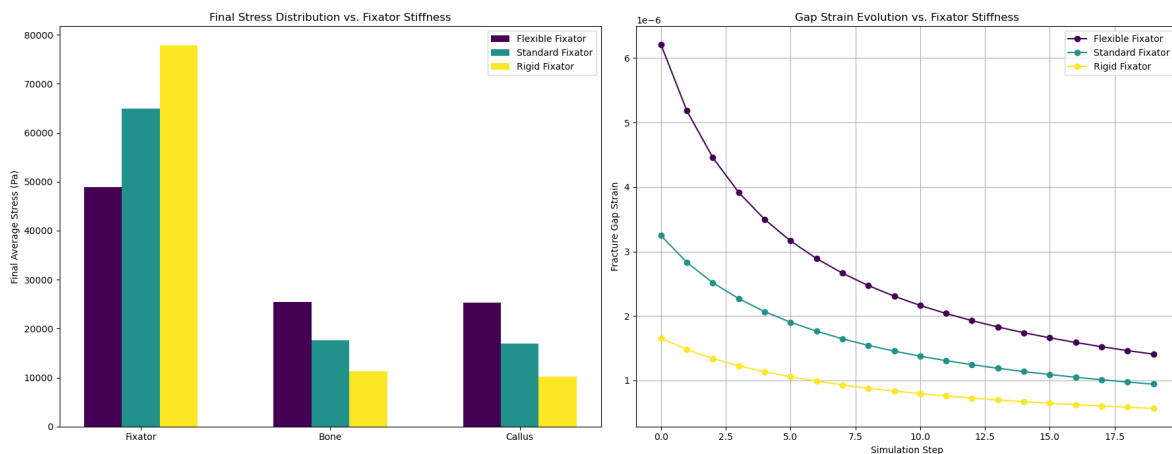

Figure 6: Parametric comparison across different fixator stiffnesses: (Left) Final average Von Mises stress distribution in the fixator, bone, and fully matured callus (Step 20). (Right) Evolution of average fracture gap strain over the 20 simulation steps for each fixator type.

7   Appendix

Wenyu Xiong: code of simulation, plot, 33% report writing

Renyi Yang: code of analysis, plot, 33% report writing

Zijian Li: code of fea-core, plot, 33% report writing

References

Gregory S. Lewis, Dominic Mischler, Hwabok Wee, J. Spence Reid, and Peter Varga. Finite element analysis of fracture fixation. *Current Osteoporosis Reports*, 19(4):403–416, 2021. doi:10.1007/s11914-021-00690-y. URL https://doi.org/10.1007/s11914-021-00690-y.

George T. Morgan, Lucas Low, Arul Ramasamy, and Spyros D. Masouros. A novel strain-based bone-fracture healing algorithm is able to predict a range of healing outcomes. *Frontiers in Bioengineering and Biotechnology*, 12:1477405, 2024. doi:10.3389/fbioe.2024.1477405. URL https://doi.org/10.3389/fbioe.2024.1477405.